

## PREPARATION AND CHARACTERIZATION OF TIN OXIDE NANOPARTICLES USING (PLAL)

WISAM J. AZIZ, RAAD S. SABRY & AHMED SADEK OTTMAN ALI

*Al-Mustansiriyah-University, College of Science, Physics Deperment, Baghdad, Iraq*

### ABSTRACT

*In this work, colloidal SnO<sub>2</sub> nanoparticles were prepared by laser ablation of tin target (purity of 99.99%) immersed in solvent (distilled water) prepared on microscope cover glass by focused beam of 532 nm of pulsed Nd:YAG laser operating at different laser pulses was varied in the range (1000-1500-2000) mJ with 1Hz repetition rate, effective beam diameter of 4.8 mm and 10 ns pulse width. Laser energy was kept constant at 700 mJ. The effects of solvents and numbe of laser pulses on the structural properties (XRD) and morphology (AFM and SEM).*

**KEYWORDS:** SnO<sub>2</sub> Nanoparticles, X-Ray Diffraction, Morphology, AFM, SEM

**Received:** Apr 27, 2016; **Accepted:** May 10, 2016; **Published:** May 23, 2016; **Paper Id.:** IJIETJUN20161

### INTRODUCTION

Nanotechnology is the application of scientific knowledge to manipulate and control matter in the nanoscale in order to make size and structure dependent properties and phenomena, as distinct from those associated with individual atoms or molecules or with bulk materials. The term “nanoscale” is defined as 1 to 100 nanometers (nm) inclusive. A microscopic particle having size at this scale is called a nanoparticle. Nanoparticles have great scientific interest as they are effectively a bridge between bulk materials and atomic or molecular structures. At this size, the substance's physical, chemical and biological properties are different from what they were at the micrometer and larger scales. By harnessing these new properties, researchers have found that they can develop materials, devices and systems that are superior to those in use today [1,2]. These unique physical, chemical and biological properties generally exist for two reasons:

- At the scale of nanometers, particles and structures have a very high surface-to-mass ratio. This makes them highly reactive compared to their bulk structure, and this reactivity can be channeled to produce superior products.
- Nanometers exist in the realm of quantum physics, and quantum properties are similarly valuable in developing enhanced materials.

There are basically two routes of making nanomaterials and nanotechnologies: a top-down approach and a bottom-up approach. The idea behind the top-down approach is the following: An operator first designs and controls a macroscale machine shop to produce an exact copy of itself, but smaller in size such as laser ablation in liquid and chemical etching. The concept of the bottom-up approach is that one starts with atoms or molecules, which build up to form larger structures such as pulse laser deposition (PLD) and physical vapor deposition (PVD). However, the top-down approach is not a friendly, inexpensive, and rapid way of producing nanostructures [3].

## EXPERIMENTAL PROCESSERS

Figure 1 shows the experimental setup for laser ablation, which includes Nd-YAG laser of 1064nm and/or 532 nm (frequency doubled) wavelength were used for laser ablation process. The ablation process is done at room temperature. The target (tin) (purity of 99.99%) has been immersed in water or aqueous solution, and fixed at bottom of glass vessel container [4].

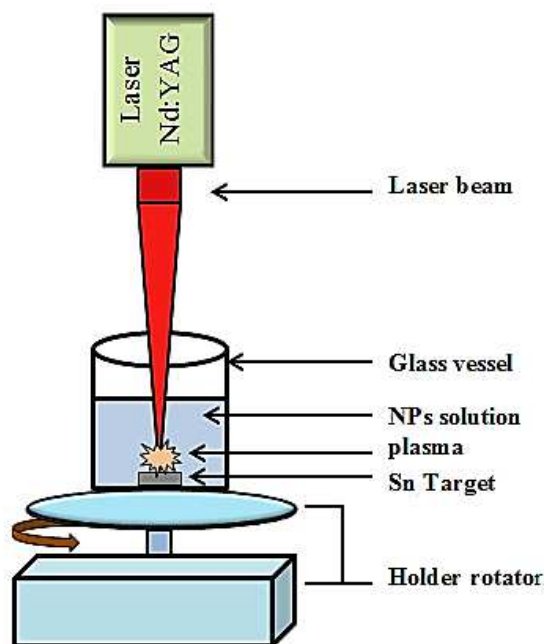


**Figure 1: Experimental Setup for Nanoparticles Synthesis by PLAL Process**

Nd:YAG laser system type HUAFEI providing pulses at 532 nm wavelength in the infrared was used for ablation of target with energy per pulse of 700 mJ, pulse duration is 10 ns, repetition rate of 1Hz and effective beam diameter of 4.8 mm, were used for laser ablation, and the number of laser pulse ranged from (1000-1500-2000) pulses have been used in this work [5].

## RESULTS AND DISCUSSIONS

X-ray diffraction (XRD) patterns of the  $\text{SnO}_2$  NPs prepared by pulsed laser ablation in DW was carried out on a dry film obtained by drop casting nanoparticles suspension on microscope cover glass substrate and evaporating the liquid media. The X-ray beam is diffracted at specific angular positions with respect to the incident beam depending on the phases of the sample [6]. Figure 2 revealed that 2 peaks with  $2\theta$  values of 26.45 and 33.43 degree, corresponding to  $\text{SnO}_2$  crystal planes of (110) and (101) respectively at 1000 pulses in DW solvent after annealing temperature at 300 C° for 20 minute.

Figure 3 revealed that 4 peaks with  $2\theta$  values of 26.601, 33.884, 37.962 and 51.801 degree, corresponding to  $\text{SnO}_2$  crystal planes of (110), (101), (200) and (211) respectively at 1500 pulses in DW solvent after annealing temperature at 300 C° for 20 minute. Figure 4 revealed that 5 peaks with  $2\theta$  values of 26.114, 33.586, 37.502, 51.608 and 56.275 degree, corresponding to  $\text{SnO}_2$  crystal planes of (110), (101), (200), (211) and (002) respectively at 2000 pulses in DW solvent after annealing temperature at 300 C° for 20 minute.

A matching of the observed and standard (hkl) planes confirmed that the product is of  $\text{SnO}_2$  having a polycrystalline in nature with tetragonal structure. Which is a good agreement with the values of (JCPDS) (Joint Committee on Powder Diffraction Standards) card no.( 41–1445), confirming the formation of  $\text{SnO}_2$  nanocrystals. XRD peaks also revealed that  $\text{SnO}_2$  nanoparticles prefer to grow in the (110) direction since the maximum intensity appeared on this direction. The crystal size of the crystalline material has an important effect in determining the properties of the material and can be estimated through the X-ray spectrum display half way to the middle of the peak (FWHM) which is given to (Debye-Scherrer relation) [7]:

$$D_g = \frac{0.9\lambda}{\beta \cos \theta_B} \quad (1)$$

Where  $D_g$ : is the crystal size, 0.9 is the Scherrer constant,  $\lambda$ : is the X-ray wavelength,  $\beta$ : is the full width at half maximum of the diffraction peak, and  $\theta_B$ : is the Bragg diffraction angle of the diffraction peaks. The average crystal size is 2.5367 nm as shown in table 2.

It has been found that the crystal size is affected by heat, As the mobility holes in the films ( $\text{SnO}_2$ ) much lower than the mobility of electrons, the increase in particle size will not lead to reducing the resistivity But lead to the removal of stresses, homogeneity as well as re-crystallization of the metal particles.

**Table 1: FWHM, (D) Crystal Size and (d) Interplane Distance of  $\text{SnO}_2$  NPs after Annealing Temperature at 1000 Pluses**

2 $\theta$ (deg.)	Plane (hkl)	FWHM (deg.)	Crystal Size (D) (nm)	d (Å)
26.45	(110)	0.26	31.4	3.349
33.43	(101)	0.51	24.6	2.64

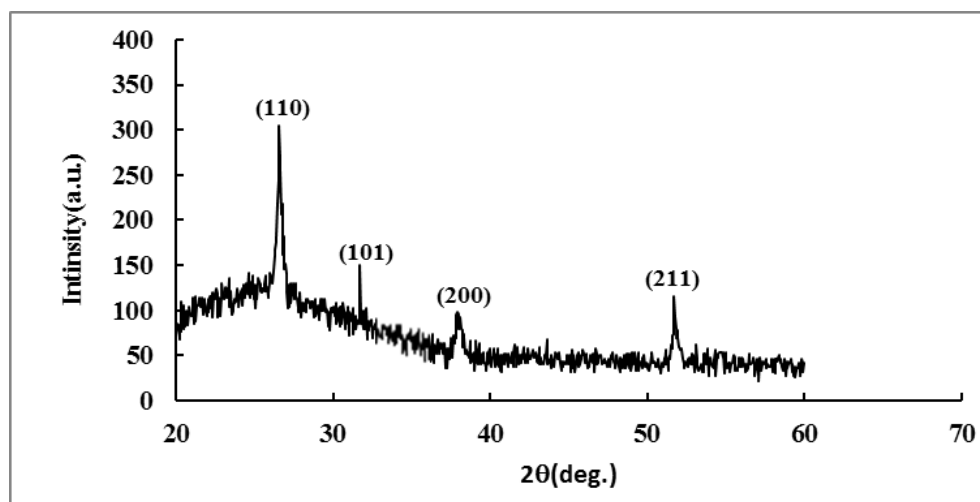


**Figure 2 : XRD Pattern of  $\text{SnO}_2$  NPs at 1000 Pulses after Annealing Temperature**

**Table 2: FWHM, (D) Crystal Size and (d) Interplane Distance of  $\text{SnO}_2$  NPs after Annealing Temperature at 1500 Pluses**

2 $\theta$ (deg.)	Plane (hkl)	FWHM (deg.)	Crystal Size (D) (nm)	d (Å)
26.601	110	1.621	18.4735	3.3579
33.884	101	0.2036	16.4982	2.6470
37.962	200	1.2507	18.6484	2.3744
51.801	211	1.403	19.9387	1.7675

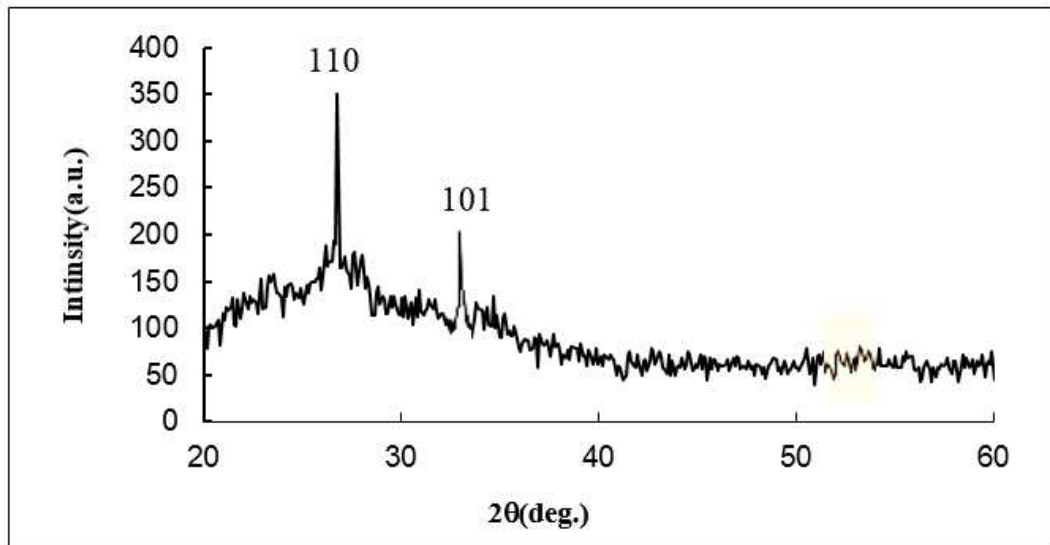


Figure 3: XRD Pattern of SnO<sub>2</sub> NPs at 1500 Pulses after Annealing Temperature

Table 3: FWHM, (D) Crystal Size and (d) Interplane Distance of SnO<sub>2</sub> NPs after Annealing Temperature at 2000 Pulses

2θ (deg.)	Plane (hkl)	FWHM (deg.)	Crystal Size (D) (nm)	d (Å°)
26.114	110	1.398	18.5	3.1479
33.586	101	0.771	31.1	2.2480
37.502	200	1.020	25.2	2.0951
51.608	211	1.152	20.5	1.3672
56.275	002	0.120	23.7	1.7640

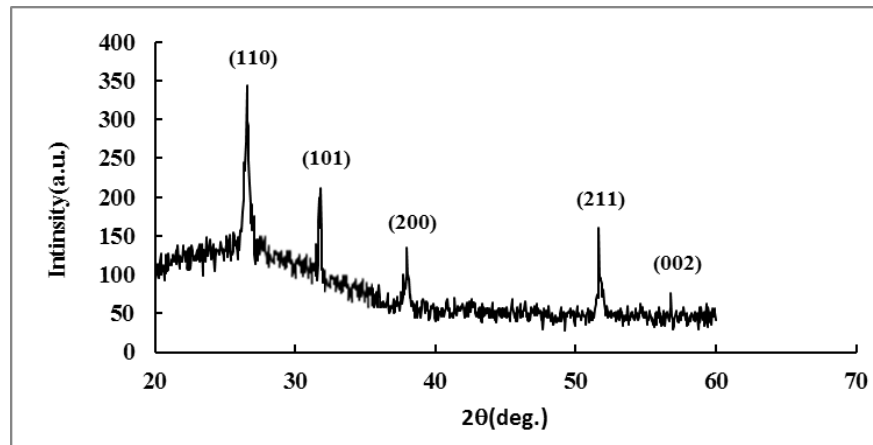


Figure 4: XRD Pattern of SnO<sub>2</sub> NPs at 2000 Pulses after Annealing Temperature

SEM images of SnO<sub>2</sub> nanoparticles prepared in (DW ,ethanol and acetone) media at same conditions of SnO<sub>2</sub> NP<sub>s</sub> are shown in figures 5. In these figures, the agglomerates are assemblies of aggregates held together by weak bonds that may be due to van der Waals forces or by ionic/covalent bonds operating over very small contact areas.

The figure 5-a shown that nanoparticles seem to irregular shape due to low number of pulses that leads to low fragmentation mechanism at initial stage from laser light compared to figure 5-b next stage at 1500 pulses which ablation and lead to a smaller nanoparticles up to 5 nm as shown in histogram, which obtain the semi-regular shape.

The figure 5-c show the nanoparticles seem to perfect spherical shape due effect the number of pulses which leads to increase the laser energy interaction with surface resulted the smaller crystalline size and homogenous surface because the long time of laser effect to fragment the area of target which lead to restructure and re-formation to give the high arrangement of partical with present the basic parameter that represented by heat combined the treatment [8].

Two mechanisms are believed to be responsible for the decrease in the nanoparticles, diameter (because of their interaction with the laser beam), which leads to the narrowing of the nanoparticles size distribution: first, the so-called Coulomb explosion phenomenon, which becomes important for highly charged NPs, where absorption of light from the nanoparticles results in the ejection of electrons into the surrounding liquid (photochemical bleaching).

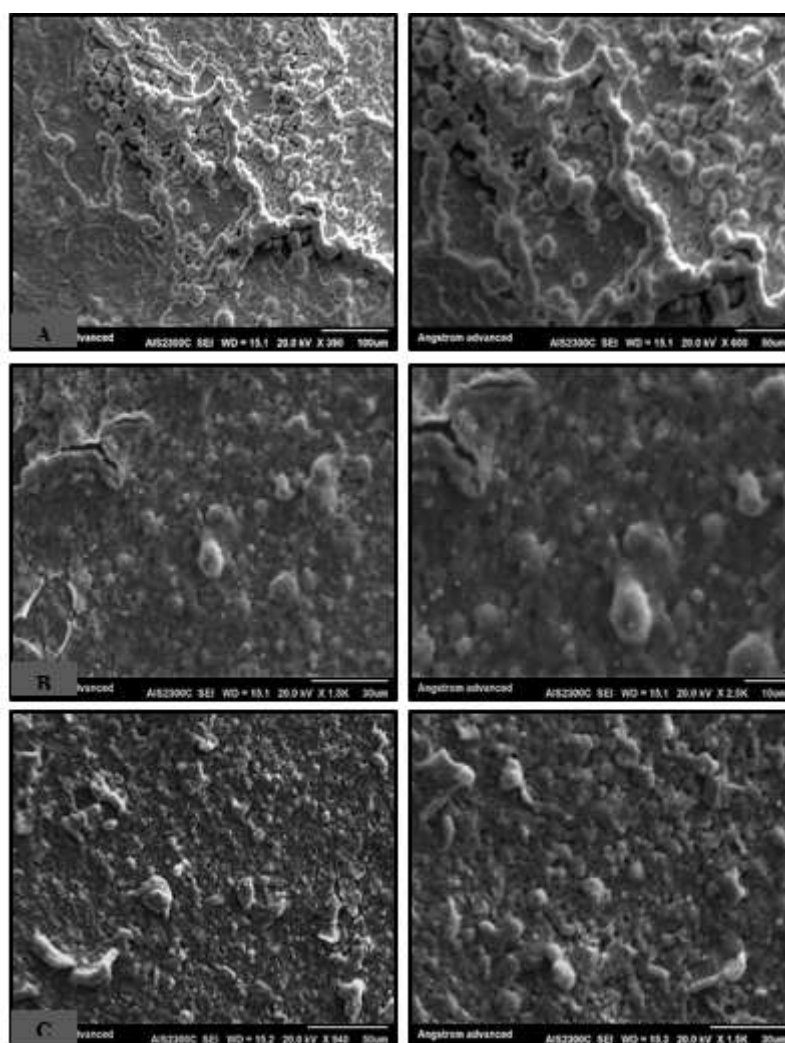


**Figure 5: SEM Images of SnO<sub>2</sub> NPs Fabricated by Ablation of Sn Target Immersed in DW Nanoparticles Prepared on Microscope Cover Glass Substrates with Pulse Laser at (A) 1000, (B) 1500 and (C) 2000 Pulses Respectively**

The surface morphology of various films has been investigated using AFM studies, which produces topological images of surfaces at very high magnification and facilitates the observation the atomic structure of crystals. AFM images, as widely known, provide a useful tool to characterize unambiguously the order of magnitude and the distribution of nanoparticle sizes. The image (6), show that SnO<sub>2</sub> nanoparticles has semi-spherical shapes and from graphical (2D and 3D) we see that the number and particles distribution increases with increasing in laser shots. It is found from this figures that



with an increase in laser shots, the size diameter of the prepared nanoparticles decreases. These results indicate that as we have increased the laser shots with time, At high number of pulses duration, relatively high number of nanoparticles screens the target, which leads to less energy absorption by it and reduction of ablation rate. Besides, primarily synthesized nanoparticles, which block the laser path, absorb a fraction of its high energy and become finer as a result of occurrence of fragmentation mechanism. Although  $\text{SnO}_2$  NPs intensely absorb UV, they also absorb IR laser beam and fragment as target absorb it and is ablated. Consequently, in end of ablation after high laser shots, average particle size significantly decreases. The occurrence of fragmentation on nanoparticles in higher ablation times and its effect on size reduction was also reported by other researchers. However, these ablated atoms and clusters tend to aggregate during or after the laser pulse [9].

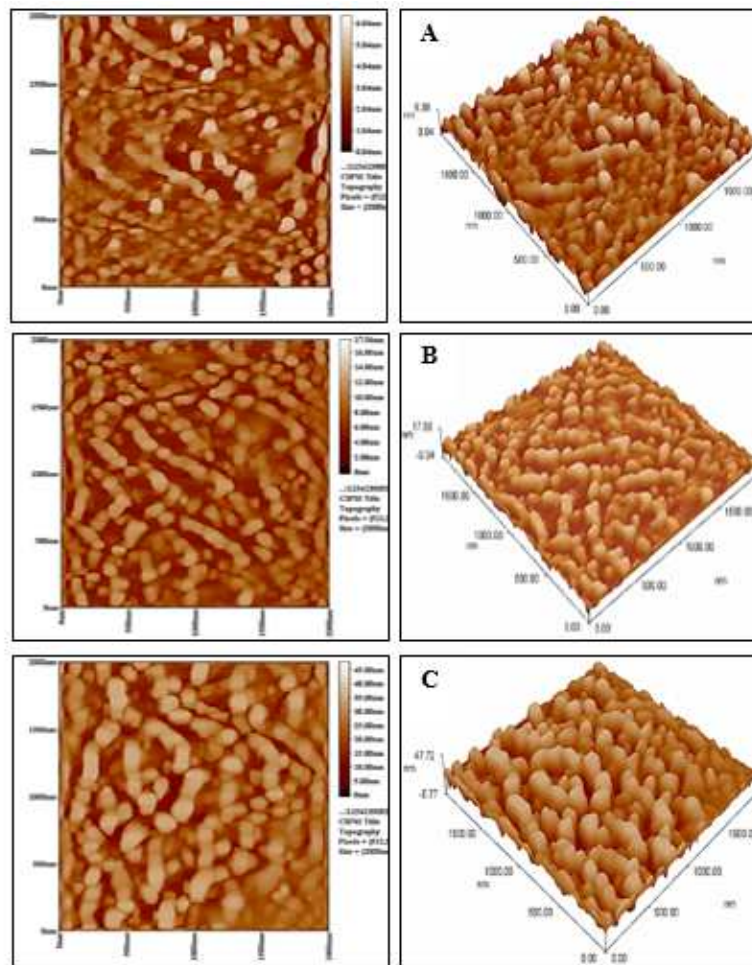


**Figure 6: Typical 2D and 3D AFM Images of  $\text{SnO}_2$  NPs Fabricated by Ablation of Sn target Immersed in DW, Prepared on Microscope Cover Glass with Pulse Shots of (A) 1000 Pulses, (B) 1500 Pulses and (C) 2000 Pulses. The Laser Energy is Kept Constant at 700 mJ**

**Table 4: Summary of the Results Observable AFM Images Morphology of  $\text{SnO}_2$  NPs on Microscope Cover Glass Substrate**

Solvent	Laser Pulses	Avg. Diameter (nm)	Ave. Roughness (nm)	RMS (nm)
DW	1000	97.91	5.48	6.51
	1500	94.53	1.89	2.19
	2000	77.54	0.715	0.859

As shown in figure 6 that but sizes of bright spherical shaped decreases with increasing the number of pulses and the its number increases with increasing number of pulses and this is proof that the size of the nanoparticles decreases with increasing number of pulses and also noted in table 4.

## CONCLUSIONS

- Laser ablation in liquid provides a simple, flexible, controllable process and less expensive way for fabrication of SnO<sub>2</sub> nanoparticles.
- From the x-ray characteristics for as-prepared samples show that amorphous structure of SnO<sub>2</sub> NPs films, but after annealing film show that is polycrystalline with tetragonal structure without any trace of an extra phase with preferential orientation in the (110) direction.
- From SEM and AFM technique the formation rate SnO<sub>2</sub> nanoparticles suspensions, mean particle size could be controlled by proper selection of the laser parameters and liquid media.
- The NPs in liquids have an almost perfect spherical shape, agglomerated and some presented chains of welded particles.

## REFERENCES

1. T.W. Kim, D.U. Lee, D.C. Choo, J.H. Kim, H.J. Kim, J.H. Jeong, M. Jung, J.H. Bahang, H.L. Park, Y.S. Yoon, J.Y. Kim, J. Phys. Chem. Solids 63 (2002) 881.
2. M.A. Gondal, Q.A. Drmash, Z.H. Yamani, M. Rashid, Synthesis of nanostructured ZnO and ZnO<sub>2</sub> by laser ablation process using third harmonic of Nd:YAG laser, Int. J. Nanoparticles 2 (2009) 142–146.
3. J. Pal, P. Chauhan, Structural and optical characterization of tin dioxide nanoparticles prepared by a surfactant mediated method, Mater. Charact. 60 (2009) 1512–1516.
4. N. Kudo, Y. Shimazaki, H. Ohkita, M. Ohoka, S. Ito, Organic–inorganic hybrid solar cells based on conducting polymer and SnO<sub>2</sub> nanoparticles chemically modified with a fullerene derivative, Solar Energy Mater. Solar Cells 91 (2007) 1243–1247.
5. David R. Lide, ed., CRC Hand book of Chemistry and Physics, CRC Press, Boca Raton, FL, 2005.
6. M. Ruske, G. Brauer, J. Pistner, U. Pfafin, J. Szczyrbowski, Properties of SnO<sub>2</sub> film prepared by DC and MF reactive sputtering, Thin Solid Films 351 (1999) 146–150.
7. Y. Ning, W. Jianhua, G. Yuzhong, Z. Xiaolong, SnO<sub>2</sub> nanofibers prepared by sol–gel template method, Rare Met. Mater. Eng. 37 (2008) 694–696.
8. G.W. Yang, Laser ablation in liquids: applications in the synthesis of nanocrystals, Prog. Mater. Sci. 52 (2007) 648–698.
9. S.H. Luo, Q. Wan, W.L. Liu, M. Zhang, Z.T. Song, C.L. Lin, Paul K. Chu, Photoluminescence properties of SnO<sub>2</sub> nanowhiskers grown by thermal evaporation, Prog. Solid State Chem. 33 (2005) 287–292.





